CONTRACTION OF RABBIT SKINNED SKELETAL MUSCLE FIBERS AT LOW LEVELS OF MAGNESIUM ADENOSINE TRIPHOSPHATE

RICHARD L. MOSS AND ROBERT A. HAWORTH
Departments of Physiology and Surgery, School of Medicine, University of Wisconsin, Madison, Wisconsin 53706

ABSTRACT The contractile properties of skinned single fibers from rabbit psoas muscle were investigated under conditions of low MgATP and no Ca^{2+} (i.e., $<10^{-8}$ M). At 1 μM MgATP, fibers shortened at a maximum velocity of 660 ± 420 Å/half sarcomere/s (n = 9), compared with 34,000 Å/half sarcomere/s measured during maximum Ca^{2+}-activation at 1 mM MgATP (Moss, R. L., 1982. *J. Muscle Res. Cell. Motil.*, 3:295–311). The observed dependence of V_{max} on pMgATP between 7.0 and 5.3 was similar to that of actomyosin ATPase measured previously by Weber, A., R. Herz, and I. Reiss (1969, *Biochemistry*, 8:2266–2270). Isometric tension was found to vary with pMgATP in a manner much like that reported by Reuben, J. P., P. W. Brandt, M. Berman, and H. Grundfest (*J. Gen. Physiol.* 1971. 57:385–407). A simple cross-bridge model was developed to simulate contractile behaviour at both high and low levels of MgATP. It was found that the pMgATP dependence of V_{max} and ATPase could be successfully modeled if the rate of detachment of the cross-bridge was made proportional to the concentration of MgATP. In the model, the similar dependence of V_{max} and ATPase on pMgATP was derived from the fact that in this range of pMgATP every pass of a cross-bridge by an actin site resulted in an attachment-detachment cycle, and every such cycle caused hydrolysis of one molecule of ATP.

INTRODUCTION

Vertebrate skeletal muscle can be placed in the state of rigor by depletion of ATP in the vicinity of the myofibrils (Bendall, 1951). Rigor is characterized by a dramatic increase in muscle stiffness (White, 1970; Mulvany, 1975) that is believed to result from the attachment of myosin cross-bridges, in the absence of ATP, to sites on the actin-containing thin filaments (Haselgrove, 1975). The onset of rigor, especially in warm muscle, is often accompanied by contracture (Bendall, 1951), a process that is not yet well characterized. Considerable evidence exists to suggest that the presence of low levels of MgATP (e.g., ~10 μM) is sufficient to induce the contracture process even in the absence of Ca^{2+}. Thus, at this level of MgATP and in the absence of Ca^{2+}, syneresis is observed to occur in isolated myofibrils (Endo, 1964), ATPase activity to persist in solutions of myosin and regulated actin (Weber et al., 1969), and tension to be developed by skinned fiber preparations (Reuben et al., 1971; Godt, 1974; Kawai and Brandt, 1976; Best, et al., 1977). One possible explanation for these findings is that the presence of rigor bonds may activate the thin filaments to allow cross-bridge cycling in the presence of MgATP at concentrations in the micromolar range (Bremel and Weber, 1972).

The present study was undertaken in an attempt to further elucidate the mechanism by which contraction occurs in the range of pMgATP between 8 and 4. As far as we are aware, no quantitative study of the kinetic properties of muscle shortening at such low MgATP concentrations has previously been undertaken. Measurements of the maximum velocity of shortening, V_{max}, as a function of pMgATP yielded a relationship that was similar in form to the previously reported actomyosin ATPase data of Weber et al. (1969) obtained in a similar pMgATP range. Using a simple cross-bridge model, we have found that this similarity of form can be explained by a common dependence of V_{max} and ATPase activity on the rate of myosin detachment from the actin filament, which in the model at low MgATP is the rate-limiting step of cross-bridge cycling. The observed pMgATP dependence of V_{max} can be successfully modeled by making the detachment rate proportional to the concentration of MgATP in this low range (<5 μM). In addition, measurements of tension in this concentration range were in substantial agreement with prior reports (e.g., Reuben et al., 1971).

METHODS

Preparation

Male New Zealand rabbits (2.6–3.2 kg body weight) were killed with a single blow at the base of the skull. The central one-third of each psoas muscle was cut free and placed in cold skinning solution containing (in millimoles per liter) K propionate, 180; EGTA, 4; ATP, 4; $MgCl_2$, 1;

imidazole, 10. The pH was 7.0 (Wood et al., 1975). Bundles of ~50 fibers were stripped free and tied to glass capillary tubes using surgical silk. The bundles were then placed in cold skinning solution containing 50% (vol/vol) glycerol, and were stored at −22°C for 3–14 d before use. On the day of its use, each bundle was cut into segments ~0.5 cm in length, which were subsequently bathed for 30 min in relaxing solution containing 0.5% (wt/vol) Brij 58 (Sigma Chemical Co., St. Louis, MO). Single fibers were dissected free in relaxing solution by simply grasping the end of a fiber and pulling it lengthwise from the bundle. Fibers having uniform striation patterns were more readily obtained with this technique than was possible with the stripping procedure used previously (Julian et al., 1981).

The fiber segments were transferred to the experimental chamber and were tied, in relaxing solution, into connectors similar to those described previously (Moss, 1979). In this study, however, titanium wire (~0.005 in. diam) was used to attach the connectors to the motor arm and force transducer element. To further lighten the connector assembly, the tubular portions of the connectors were removed and the remaining troughs were attached with epoxy directly to the titanium wires. Fiber segments between 0.7 and 1.6 mm in length remained exposed to the bathing solution between the connectors. During experimental procedures, the segments were viewed and photographed through a microscope (Moss, 1979) to ensure that the striation patterns were uniform along the length of each segment and to obtain measurements of the mean sarcomere length. The initial sarcomere length in relaxing solution was set to 2.4–2.6 μm by adjusting the overall length of the segment.

Solutions

The solutions used were in general similar to those described by Julian (1971). Relaxing solution contained (in millimoles per liter): KCl, 100; EGTA, 2; $MgCl_2$, 1; ATP, 4; imidazole, 10. The pH was 7.0. In several instances, a Ca^{2+}-containing activating solution of pCa 5.49 was used to obtain a measure of the tension-generating capabilities of the fiber segments. This solution was similar to relaxing solution except that the total concentrations of EGTA and Ca^{2+} were 4 and 3.8 mM, respectively. The apparent stability constant for the Ca-EGTA complex was assumed to be $10^{6.68}$ (Julian, 1971).

Solutions in which the pMgATP was varied always contained $MgCl_2$ at a total concentration of 1 mM. Thus, variations in pMgATP were accomplished by varying the total concentration of added ATP using the relevant pK's and stability constants listed in Sillen and Martell (1964). The concentration of ATP in these solutions was buffered by the addition of creatine-phosphokinase (Sigma Chemical Co.) to a final concentration of 1 mg/ml, and creatine-PO_4 (14.5 mM), as described by Godt (1974). All experimental measurements were done at a solution temperature of 25°C.

Mechanical Apparatus

The experimental chamber and associated apparatus have been described previously (Moss, 1979; Julian and Moss, 1981), though several changes have been made for the present study. The scanning motor (model 300s; Cambridge Technology, Inc., Cambridge, MA) that was used could be adjusted to achieve a 0–100% length step-response time of 0.6 ms, when the motor arm and connecting structure were attached to the fiber segment. The force transducer was a semiconductor strain-gauge device (model AE801; Aksjeselskapet Mikro-Elektronikk, Horten, Norway) having a resonant frequency of 1.2 kHz; the connecting wire was attached to the fiber segment, and the sensitivity could be varied between 2.5 and 7.5 mV/mg. A wheatstone bridge in conjunction with an instrumentation amplifier (model AD520J; Analog Devices, Inc., Norwood, MA) was used to detect and amplify force changes. Peak-to-peak noise at the amplifier output was equivalent to 0.5 mg. The transducer element was encased in a stainless steel cyclinder designed to strain limit the element and to prevent water damage. A slot was cut into the side of the cylinder to allow passage of a titanium connecting wire (~0.005 in. diam) from the element to the fiber segment. The length and force signals were recorded on a digital oscilloscope (model 2090-3B, Nicolet Instrument Corp., Madison, WI) and were stored on magnetic disk for later analysis.

Measurement of the force-velocity properties of the fiber segments using load steps was done using a switching network (Isotonic Linking Circuit, drawing 0197; Cambridge Technology, Inc.) designed by Mr. Bruce Rohr. The output of this circuit was fed into the position input of the model 300s ergometer. Examples of the records that were obtained are shown in Fig. 2. A notable feature of these records is that the load under which the muscle shortened was constant in each instance. In addition, the force changes in response to the load steps were rapidly attained with minimal oscillation in the servo system.

Experimental Procedures

At the beginning of each series of mechanical measurements, the fiber segments were put into rigor by transferring them from relaxing solution into rigor solution, which was similar to relaxing solution but contained no added Mg^{2+} or ATP. To ensure complete washout of these constituents, the rigor solution was changed every 2 min for a total soak time of 6 min. Still longer soak times resulted in no further changes in the steady isometric tension. The segment was then placed in rigor solution containing added creatine-PO_4 and creatine-phosphokinase, before being transferred to solutions containing controlled amounts of MgATP. Mechanical measurements were made in each preparation at several pMgATP levels. In most instances, following mechanical measurements at a particular pMgATP, the segment was returned to relaxing solution and then reequilibrated to the zero Mg^{2+} and ATP solutions before being transferred to a solution containing a different pMgATP. In a few cases, especially those involving tension measurements at pMgATP > 7.0, the fiber was successively transferred to solutions of lower pMgATP without intervening periods of reequilibration. Control measurements of tension in rigor solution were made following every two or three test measurements. If either of these parameters was found to have declined by >10% of the originally measured values, the fiber segment and the data of the prior test series were discarded. Segments were also discarded if regions of gross striation nonuniformity were observed anywhere along the length of the segment.

Measurements of tension or of V_{max} and tension were obtained during any one activation of a segment at a particular pMgATP. Isometric tension was measured during steady tension development by rapidly (i.e., step complete within 0.7 ms) introducing slack into the muscle, thereby reducing tension to zero. This procedure permitted an accurate measure of tension by avoiding the effects of possible tension baseline drift during the period of tension development.

V_{max} was measured using the load-stepping technique, which was previously described in detail (Julian and Moss, 1981). Once a steady tension was established, a series of one, two, or three progressively lighter loads were applied (Fig. 2). The steady velocity obtained at any given load was found not to vary when measured singly or as part of a series of two or three load steps, a finding similar to that reported by Julian (1971) in Ca^{2+}-activated muscle fibers from the frog.

Data Analysis

The isometric tension data were normalized to segment cross-sectional area using the method of Gordon et al. (1966), and were expressed in units of kilograms per square centimeter. The measured velocities were expressed in muscle lengths (ML) per second, which was calculated by dividing the absolute velocity (in millimeters per second) by the length of the segment (in millimeters) measured at an average sarcomere length of 2.4 μm (Julian and Moss, 1981). An estimate of V_{max} was obtained by fitting a linearized hyperbola (Katz, 1939) to the measured force-velocity data, and extrapolating the fitted line to zero relative load (Julian and Moss, 1981). The data points used for fitting were obtained in a range of relative loads between 0.02 and 0.40 of P_o. These data were in general well fit by a hyperbolic function, though there was no a priori reason to believe

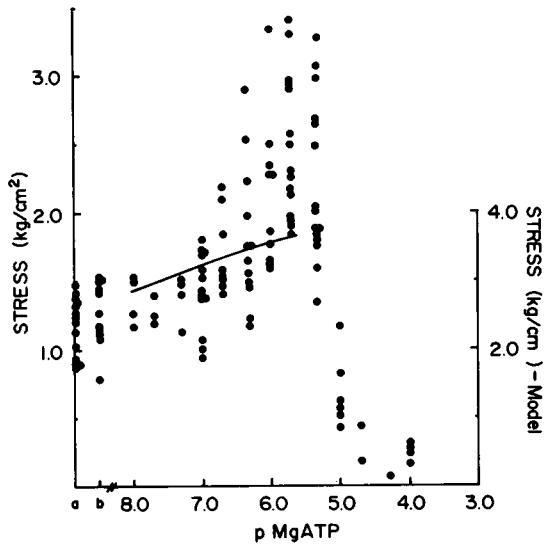

FIGURE 1 Stress plotted as a function of pMgATP. *a*, indicated on the abscissa, represents no added ATP, i.e., rigor solution; *b* represents rigor solution with CP-CPK added as described in Methods. The solid curve is the stress-pMgATP relationship calculated from the model (Note that the ordinal scale for the model is different from that for the data obtained from the fiber segments.) In several instances, individual data points were displaced laterally a small amount to avoid superimposition.

that this would be so. At relative loads >0.40, the measured velocities were usually <0.005 ML/s, which were difficult to measured accurately. These data points were thus excluded from the analysis and calculation to obtain V_{max}. Calculations involving the cross-bridge model were done using a Texas Instruments TI 59 programmable calculator and printer.

RESULTS

Isometric Tension

The rigor tensions obtained in different fiber segments (Fig. 1) ranged between 0.85 and 1.48 kg/cm^2, with a mean value of 1.17 ± 0.21 kg/cm^2 (SD, n = 14). Subsequent transfer of the segments into rigor solution containing the creatine phosphokinase– (CPK–) creatine-PO_4 (CP) regenerating system most often resulted in small, though statistically significant, increases in isometric tension ($P < 0.05$; paired t-test; n = 10), the mean value being 1.23 ± 0.08 kg/cm^2 (n = 10). This small effect of the regenerating system upon tension development indicates that there was little carryover of ATP or ADP from the relaxing to the rigor solutions.

Tension was found to vary markedly when the pMgATP of the bathing solution was altered (Fig. 1). As the pMgATP was decreased from 8.0 to 7.0, virtually no changes in mean tension relative to that in rigor solution were measured, though in three-fiber segments, slight increases in tension at a pMgATP of 7.00 were observed. Below 7.00, mean tension increased progressively, reaching a maximum value of 2.49 ± 0.52 kg/cm^2 (SD, n = 15) at a pMgATP of 5.75. While all fiber segments demonstrated a tension increase in this pMgATP range (Fig. 1), for several fibers this increase was only a few percent of the tension developed at pMgATP 7.0. The pMgATP value for the occurrence of maximum tension varied in individual fibers between 6.00 and 5.25. As the pMgATP was lowered

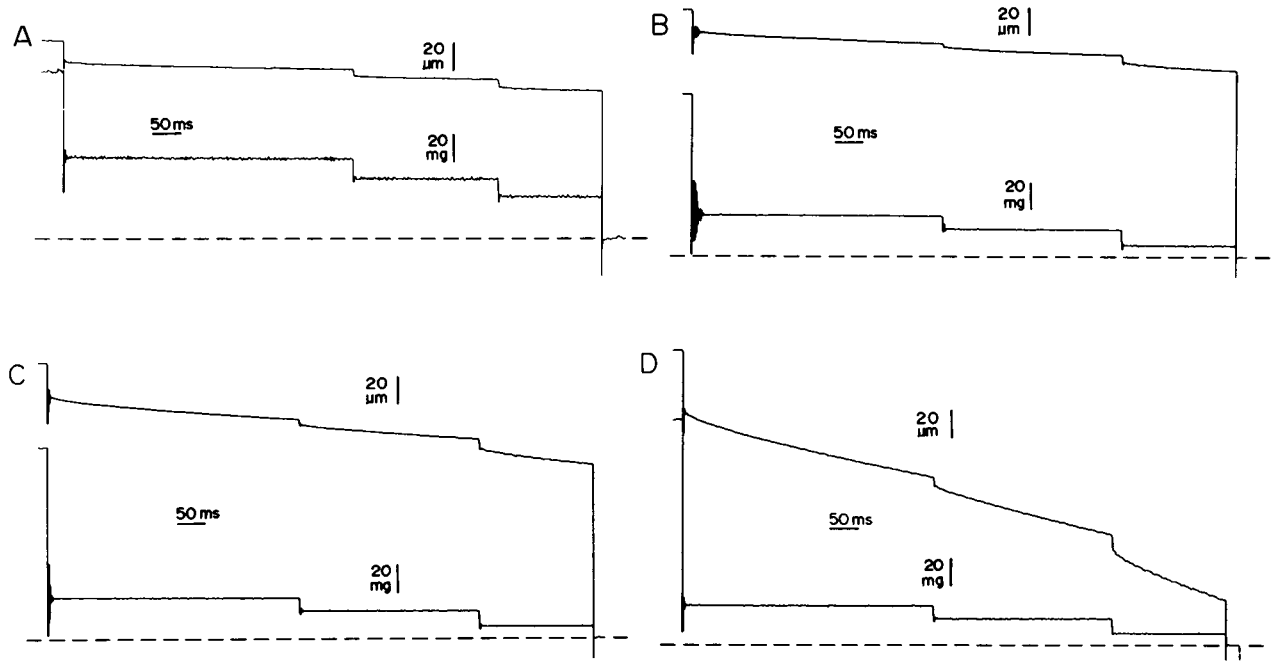

FIGURE 2 Records of tension and length obtained during force-velocity measurements at various concentrations of MgATP. In each instance, the *upper* trace is length and the *lower* is tension. Each measurement was obtained from the same fiber segment at the following MgATP concentrations: (*A*) 0 µM (i.e., rigor solution with added CP-CPK); (*B*) 1.0 µM; (*C*) 2.0 µM; (*D*) 5.0 µM. The dashed lines (---) in each case represent the zero-force baseline. Fiber No. 4156; *ML* = 1.46 mm; *SL* = 2.5 µM.

further, tension declined rapidly from the maximum, finally reaching, at pMgATP 4.50–4.00, values corresponding to those measured in relaxed fibers.

Maximum Shortening Velocity (V_{max})

A record of the length changes obtained during loadsteps imposed while in the rigor solution containing CPK and CP is shown in Fig. 2 *a* for one fiber preparation. As would be expected for a fiber in rigor, virtually no shortening could be seen under load, a finding that provided substantiating evidence that adenine nucleotides were not present in significant amounts. However, upon placing the fiber segments into a solution of lower pMgATP (Fig. 2 *b–d*), load steps applied during steady tension development resulted in marked shortening. At each progressively lighter load, the segments first underwent a period of shortening in which the velocity continually decreased from an initially high value, before finally attaining a constant shortening velocity. A novel feature of the velocity measurements at high pMgATP compared with those previously obtained at low pMgATP (Moss, 1982) is the rather slow rate of adjustment to a new steady state velocity following a step change in load (Fig. 2). We do not at present have an explanation for this phenomenon. The steady velocity was in each case taken to be characteristic of the relative load and pMgATP under which it was obtained. Plots of force-velocity data points are shown in Fig. 3 for a single preparation activated at several different pMgATP levels (see Discussion for details of curves). Clearly, the force-velocity relation of this segment became progressively elevated as the pMgATP was decreased. These data were fitted using the linearized force-velocity hyperbola (Katz, 1939), and the ordinal intercept of the fitted line at zero relative load was used to estimate V_{max}. In this instance, V_{max} increased from 0.012 ML/s at a pMgATP of 7.00 to 0.117 ML/s at 5.30. The V_{max} data obtained from all fiber segments are shown in Fig. 4, in which, due to the variability in the V_{max} values measured at the lower pMgATP levels, V_{max} is expressed as a fraction of the V_{max} measured in the same fiber at pMgATP 6.0, the only value at which V_{max} was measured in all the segments. As pMgATP was decreased from 7.0 to 5.3, there was a ~10-fold increase in the mean V_{max} value. It was not possible to obtain reliable V_{max} values at still lower pMgATP, due to the appearance of striation nonuniformities at both 5.0 and 4.7. The immediate cause of the nonuniformity was not clear; however, to attain these pMgATP levels, the fiber segments had to pass through higher pMgATP levels due to the dilution of the rigor solution within the fiber by the test solution in the bath. Thus, while the steady tensions at pMgATP of 5.0 and less are relatively small, the segments generated large transient tensions during the period of equilibration. Final attainment of a steady tension took as long as 3 min, during which time a gradual deterioration in the fiber could occur due to, for example, enhancement of initially small striation nonuniformities. Several attempts were made in which the fiber was first bathed in relaxing solution (4 mM ATP) that was subsequently diluted to the desired pMgATP. This procedure also resulted in long times to establish steady tensions, and nonuniformities were consistently observed to occur. Velocity records at pMgATP 5.0 were curvilinear, precluding measurement of a unique velocity value; however, at any given load, even the lowest velocity attained during the time course of shortening was greater than the steady velocity measured at higher pMgATP levels and the same relative load.

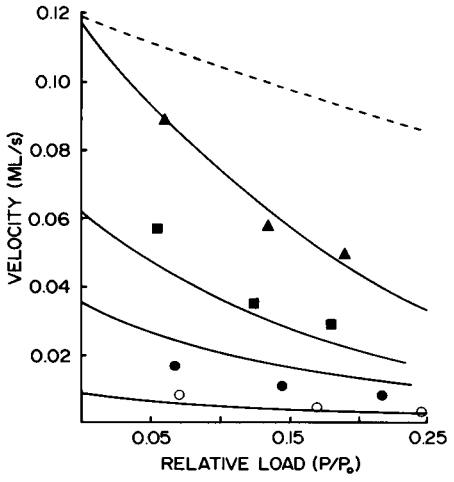

FIGURE 3 Velocity plotted vs. relative load. Raw velocity data are plotted for a single fiber segment at 5 μM (▲), 2 μM (■), 1 μM (●), and 0.1 μM (○) MgATP. The solid lines (—) are the relative velocity–relative load curves predicted by the model. The dashed line (---) is the predicted curve obtained at 5 μM MgATP by making g independent of x, as explained in text.

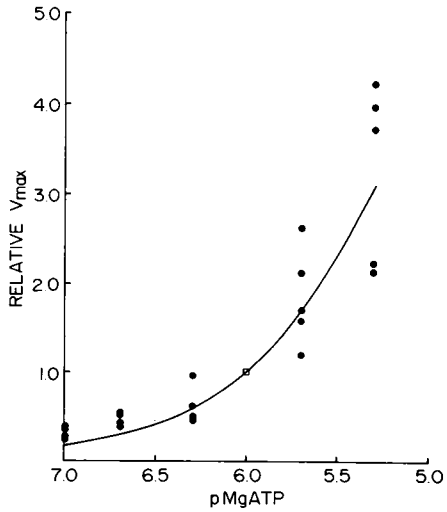

FIGURE 4 Plot of V_{max} vs. pMgATP. In each fiber, V_{max} values obtained at the various MgATP levels were scaled to V_{max} in the same fiber at pMgATP = 6.0 (□). The solid line (—) is the relative V_{max}-pMgATP relation predicted by the model.

DISCUSSION

It is reasonable to think of the rigor state as just one state in the normal cross-bridge cycle whose duration is very short when MgATP is readily available. We have therefore attempted to model the observed shortening characteristics at low MgATP levels by an adaptation of a simple model for steady state cross-bridge interaction with the actin filament (Hill and White, 1968).

Cross-bridge Model

The muscle contraction was modeled using a three-state, one-way cycle involving ATP hydrolysis, plus equilibria with a fourth state in which myosin is ATP-deficient (Fig. 5). The following rate functions were used:

$$f = C_1 \exp\left[-(x - 80)^2/2\sigma_1^2\right]$$

$$K = C_2[1 - \arctan(x/b)/90]$$

$$g = C_3 S \exp\left[(x - 80)^2/2\sigma_2^2\right]$$

$$a_1 = C_4 \exp\left[x^2/2\sigma_4^2\right]$$

$$a_{-1} = C_5 \exp\left[-x^2/2\sigma_3^2\right]$$

$$K_S = \text{constant, independent of } x$$

where x is the displacement (in ångströms) of an attached actin from the minimum free energy position of the attached cross-bridge; S is the concentration of MgATP, and C_1, σ_1, C_2, b, C_3, σ_2, C_4, C_5, and σ_3 are constants. The x dependence of these functions is shown in Fig. 6 for the values of constants given in Table I. It may be seen that the model centers around a cross-bridge detachment rate (g) that is made proportional to the concentration of MgATP. The influence of head position and strain in the cross-bridge link on attachment rate is modeled by giving f a bell-shaped dependence on x, as others have done (Hill and White, 1968; Eisenberg et al., 1980), with the optimal position for attachment at $x = 80$ Å. After passing quickly to the major force-producing state (included in state 1), the cross-bridge loses bound nucleotides at the rate given by K, which increases as x becomes smaller. Thus, state 1 includes all states of the attached cross-bridge with bound

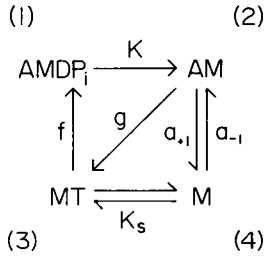

FIGURE 5 Relationship between cross-bridge states. State 1, myosin bound to actin, with nucleotide bound; state 2, myosin bound to actin, no nucleotide bound; state 3, free myosin with nucleotide bound; state 4, free myosin, no nucleotide bound. The rate functions between states are defined in text.

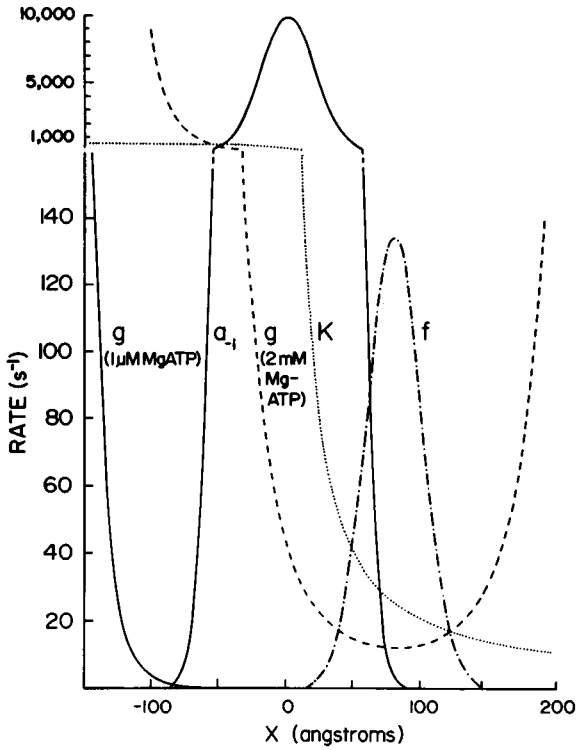

FIGURE 6 Variation of the rate functions with x. Values for the constants shown in Table I were used. The magnitude of a_1 was too small to show on this scale.

nucleotides. These states are telescoped together here, because under conditions of low MgATP they are less significant kinetically than at high MgATP. Release of nucleotides leaves the cross-bridge in state 2 (Fig. 5), where it is susceptible to release by MgATP at the rate g. At high MgATP the cross-bridge release rate is essentially governed by the maximal value of K, which occurs at negative x (Fig. 6). The form chosen for K is similar to that used by Eisenberg et al. (1980) for the cross-bridge release rate at high MgATP. The step of ATP binding and cross-bridge release, which is not usually included explic-

TABLE I
NUMERICAL VALUES OF CONSTANTS USED IN RATE EQUATIONS

Constant	Value
C_1	135 s^{-1}
C_2	320 s^{-1}
C_3	6,000 s^{-1} M^{-1}
C_4	0.01 s^{-1}
C_5	10,000 s^{-1}
b	10 Å
σ_1	20 Å
σ_2	50 Å
σ_3	20 Å
σ_4	50 Å
K_S	10^{-11} M
d	380 Å

itly, is given here by the rate g, which is not rate limiting at high MgATP but becomes so at low MgATP. The rationale for the form chosen for g is given later. State 3 includes all states of the free cross-bridge with nucleotide bound. Binding of the nucleotide free cross-bridge (state 4, Fig. 5) is given by the rates a_1 and a_{-1}. These were chosen such that the strongest binding position was at $x = 0$, corresponding to the 45° position of decorated actin (Spudich et al., 1972). The high value of C_5/C_4 reflects the strength of binding of nucleotide-free myosin to actin at $x = 0$ (Marston and Weber, 1975). The exponential form gives a linear force-displacement relationship. The value chosen for K_S is similar to that found for ATP binding to S1 (Goody et al., 1977). Following the original concept of Huxley (1957), the fraction n of cross-bridges in each state is governed by the equations

$$-v\frac{dn_1}{dx} = fn_3 - Kn_1$$

$$-v\frac{dn_2}{dx} = Kn_1 + a_{-1}n_4 - (g + a_1)n_2$$

$$n_1 + n_2 + n_3 + n_4 = 1$$

$$K_S = n_4 S/n_3$$

where v is dx/dt. These equations combine to give

$$-v\frac{dn_1}{dx} = -(f^1 + K)n_1 - f^1 n_2 + f^1 \quad (1)$$

$$-v\frac{dn_2}{dx} = (K + a^1_{-1})n_1 - (a^1_{-1} + a_1 + g)n_2 + a^1_{-1} \quad (2)$$

where $f^1 = fS/(S + K_S)$ and $a^1_{-1} = a_{-1}K_S/(S + K_S)$.

These equations were solved for n and n_2 by numerical approximation at 5-Å intervals. The n values were used to calculate the following parameters:

$$\text{force} = \frac{2kT}{d}\int_{-d/2}^{+d/2}\left[\frac{n_1}{\sigma_1^2} + n_2\left(\frac{1}{2\sigma_3^2} + \frac{1}{2\sigma_4^2}\right)\right]\cdot x \cdot dx$$

where k = Boltzman's constant and T = absolute temperature. This formulation of force assumes that all cross-bridges in state 1 exert a force proportional to x; that is, on attachment the transition to the major force-producing state is very rapid. Moreover, we have arbitrarily used σ_1 to characterize the stiffness of this state. Force calculated by this equation was converted to dynes per square centimeter by multiplication by the number of cross-bridges per square centimeter per half sarcomere: values of 8.4×10^{16} cross-bridges/cm^3 (Ebashi et al., 1969) and a half sarcomere length of 1.20×10^{-4} cm were used.

For ATPase,

$$\text{ATPase} = \frac{1}{d}\int_{-d/2}^{+d/2} n_1 K\,dx$$

$$= \frac{1}{d}\int_{-d/2}^{+d/2} n_2 g\,dx.$$

The equality of these two values for the ATPase was used as a check of the accuracy of computation. For ATP binding to the cross-bridge, the fraction with ATP bound = $1/d\int_{-d/2}^{+d/2}(1 - n_2 - n_4)dx$. Under the conditions employed here (K_S very small), n_4 was sufficiently small to be ignored in this integral. Finally, the mean number of completed cycles (r) per pass of an actin site past a given cross-bridge was found from r = ATPase · d/v (Eisenberg et al., 1980). Calculations were performed for various values of v and S, and using the values of the constants given in Table I.

Contractile Properties at High [Mg ATP]

At [Mg ATP] = 2 mM the detachment rate function g is high, so that the actual detachment rate is controlled for the most part by the function K, which is very similar to the detachment rate function used by Eisenberg et al. (1980). The values of F_o and V_{max} are given in Table II and the force-velocity curve is shown in Fig. 7, together with experimental data taken from Moss (1982). The fit is quite good, largely through judicious choice of C_2 (which determines the shape of the force-velocity curve; see Eisenberg et al., 1980). In addition, it is seen from Table II that reduction of the level of MgATP to 0.3 mM, still a relatively high level, produces a significant reduction in the predicted level of V_{max}. Such an effect has in fact been observed by Ferenczi et al. (1979) for Ca^{2+}-activated contractions in skeletal muscle fibers of the frog. Values for n_1 and n_2 at different values of x are shown in Fig. 8 for a fiber contracting at V_{max}. Two features are noteworthy. First, at high [MgATP] not many cross-bridges are attached. Because $n_1 + n_2 = 0.95$ at $x = 80$ Å for a fiber under isometric contraction, this model at high levels of MgATP is of the type where the reduced force at high velocity is caused principally by a reduction in the fraction of attached cross-bridges (Eisenberg et al., 1980). This is also reflected in the low value of r at V_{max} (Table II).

TABLE II
COMPARISON OF SOME EXPERIMENTAL AND PREDICTED CONTRACTION PARAMETERS

Contraction parameter	Theoretical	Experimental
At 2 mM Mg ATP		
Isometric force (kg/cm^2)	3.15	1.77 ± 0.33 (Moss, 1982)
Maximum velocity (Å/half-sarcomere/s)	33,967	34,020 ± 13,600 (Moss, 1982)
No. of cycles per pass (r) at V_{max}	0.17	
At 0.3 mM Mg ATP		
Maximum velocity (Å/half-sarcomere/s)	23,349	
At 1 μM Mg ATP		
Maximum velocity (Å/half-sarcomere/s)	670	661.5 ± 418
No. of cycles per pass (r) at V_{max}	1.002	

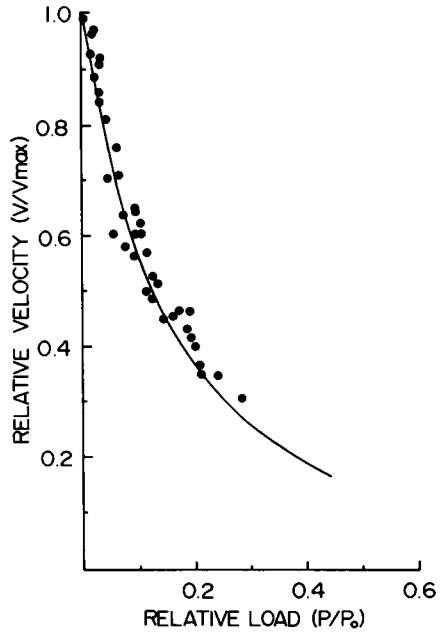

FIGURE 7 Force-velocity curve of psoas muscle at high levels of MgATP (2 mM). Data points are taken from Moss (1982). Solid curve (—): force-velocity curve derived from the model. Values for V_{max} and P_o are given in Table I.

Second, even at this high level of MgATP, a significant fraction of the attached cross-bridges is in state 2. This is because we have made the detachment function, g, x dependent (see below), so that at x values near 80 Å the detachment rate is not great, even at high MgATP levels. This accounts for the effect on V_{max} of reducing MgATP from 2 to 0.3 mM (Table II).

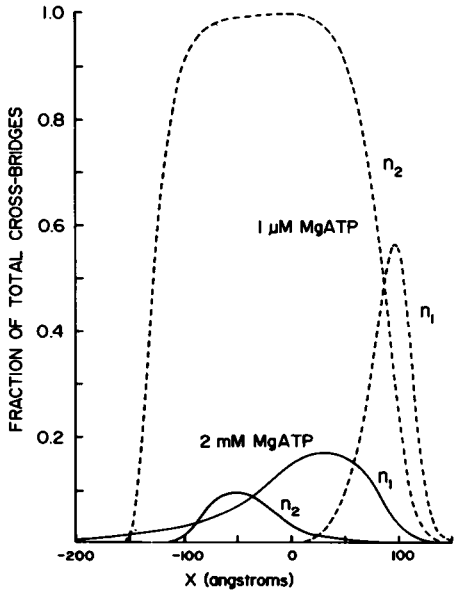

FIGURE 8 Fraction of cross-bridges in states 1 and 2 at different values of x. Curves predicted by the model are shown for high and low values of MgATP concentration.

Contractile Properties at Low [MgATP]

V_{max}. At low [MgATP] the function g becomes rate limiting for detachment, and V_{max} at any S is determined principally by C_3 and σ_2. These were therefore chosen to fit the V_{max} found at a single low value of S (Table II). The model also gave a reasonable fit for V_{max} as a function of pMgATP (solid curve, Fig. 4). The shape of this curve results mostly from our having made the function g proportional to the concentration of MgATP. The good fit with the experimental data therefore indicates that the rate of shortening of fibers in this range of pMgATP can be accounted for in terms of the cross-bridge detachment rate being rate limiting, and being proportional to [MgATP].

An alternative explanation for the [MgATP] dependence of V_{max} should be considered. If the ATP-regenerating system was excluded from the fiber, the rate of diffusion of regenerated MgATP into the fiber could limit its availability for contraction. However, there is no reason to suppose that the skinned fiber would exclude creatine phosphokinase. The ability of myosin antibody to permeate myofibrils (Guerriero et al., 1981) suggests that creatine phosphokinase will also permeate myofibrils. Moreover, higher levels of creatine phosphate and creatine phosphokinase did not increase the rate of contraction at any given ATP level, showing that ATP regeneration was not limited by this system. This is in accord with others who have previously used this system (Godt, 1974; Maruyama and Weber, 1972).

Force-Velocity Curve. The solid curves in Fig. 3 show the force-velocity curves predicted by the model at several low values of [MgATP]. The parameters listed in Table I were used, except that a value of C_3 = 3,400 was used to fit the V_{max} at 5 μM ATP for this particular fiber. It is seen that the shape of the force-velocity curve is well fit by the model, though the experimental data for 1 and 2 μM ATP were displaced from the theoretical curves. That these displacements were not for the most part systematic is illustrated by the V_{max} data in Fig. 4: when the 1 μM ATP data from all fibers were normalized, the 2 μM data were distributed around the theoretical curve. The shape of the force-velocity curve was determined principally by the x dependence of the function g. If g was made independent of x by setting $g = C_3S$, and C_3 was increased to give almost the same V_{max} value as before, the force-velocity curve shown by the dashed line in Fig. 4 was predicted for 5 μM MgATP. This curve is almost linear, dropping to $V_{max}/2$ near P/P_o = 0.5. An acceptable shape can be modeled using any function for g that increases strongly as x becomes negative. We have chosen this particular one to be consistent with the suggestion of Eisenberg and Green (1980) that the detachment rate of myosin-ATP from the actin filament is small around x = 80 Å, and increases as the cross-bridge is rotated.

Isometric Force, P_o. The variations in tension that were observed in the present study as the pMgATP was varied between 8.0 and 4.0 are qualitatively similar to the results of previous studies involving skinned preparations from crayfish walking muscles (Reuben et al., 1971; Kawai and Brandt, 1976), rat ventricle (Fabiato and Fabiato, 1975), and vertebrate skeletal muscles (Godt, 1974; Fabiato and Fabiato, 1975). In each instance, tension was found to increase as the pMgATP was lowered from 8.0. At ~6.0, tension reached a maximum, which was followed by a rapid decline as the pMgATP was further decreased. The predicted values for P_0 are shown by the solid line in Fig. 1. The predicted values are somewhat high, for two possible reasons: (*a*) our method of approximation, making all state 1 cross-bridges exert force proportional to x, introduces an overestimation of P_0, or (*b*) the value of P_0 measured may be too low. Kawai and Brandt (1976) suggested on the basis of tension and stiffness measurements on skinned crayfish fibers that cross-bridges exhibit two rigor states. Cross-bridges that are under strain, as during a Ca^{2+}-activated contraction, prior to induction of rigor appear to be stiffer and to generate more tension than cross-bridges in the relaxed state prior to rigor. Kawai and Brandt (1976) hypothesized that low-rigor bridges are formed by dissociation of MgATP from free myosin that then interacts with actin, resulting in less tension than high-rigor bridges that are formed by dissociation of nucleotide from attached (force-generating) cross-bridges. In the present study, development of rigor from the relaxed state resulted in tensions that varied over a wide range. This indicates that the low-rigor state, if such exists in rabbit skeletal muscle, is difficult to define. Rather than postulate a unique cross-bridge state to describe this behavior, it may be possible to explain at least part of the difference in the tensions associated with the low and high rigor states in terms of a mechanical artifact of the skinned fiber preparation. Because the ends of a skinned fiber are usually compressed or crushed by the attachment to the apparatus, these preparations possess a relatively high degree of end compliance (Julian et al., 1981). In transferring a skinned fiber from a relaxing to a rigor-inducing solution, cross-bridges undergoing a single attachment and power stroke would not cause sufficient internal shortening to stretch the compliant ends. The preparation would therefore appear relatively compliant and would transmit only a small amount of tension to its ends. By activating cross-bridges with calcium prior to rigor, the compliant regions at the ends would be extended during tension development by internal shortening resulting from the cyclic attachment and detachment of the cross-bridges. With subsequent induction of rigor, the now-strained ends of the preparation would be able to sustain the tension generated by the cross-bridges. Also, since biological tissues generally have nonlinear tension-extension characteristics (Fung, 1967), the stiffness of the end regions would be much greater than if pre-straining had not occurred. Thus, preparations in rigor following prior activation with Ca^{2+} would generate greater tension and be stiffer than preparations without prior activation. Skinned muscle fibers have been shown to vary in the degree to which the ends are compliant (Julian et al., 1981). Thus, in regard to the data of the present study, the observed variations in tension when the fibers were placed in rigor solution would, at least in part, reflect differences in the amount of end compliance from fiber to fiber, and the measured values at low MgATP are probably underestimates of the true values. The drop in P_0 seen at higher levels of [MgATP] will not be predicted by the model, since the model assumes that all the actin units are switched on: the observed decline in P_0 is presumably caused by the switching off of actin units by loss of rigor bonds (Bremel and Weber, 1972).

ATPase. The shape of the predicted ATPase curve as a function of pMgATP is similar to that of the V_{max} curve (Fig. 4), and is also similar (Fig. 9) to the measured ATPase activity of myofilaments as measured by Weber et al. (1969). The origin of the similarity between the V_{max} dependence on pMgATP and that of ATPase is their common dependence on the rate-limiting detachment function g. The cause of this common dependence is evident from Table II. In contrast to the situation at high levels of MgATP, the value of r at V_{max} at low levels of MgATP is very close to unity. This means that every pass of a cross-bridge by an actin site results in an attachment-detachment cycle and the hydrolysis of one molecule of ATP. Any velocity of contraction must therefore be matched by a parallel rate of ATP hydrolysis. A correspondence between the magnitude of the Ca^{2+}-

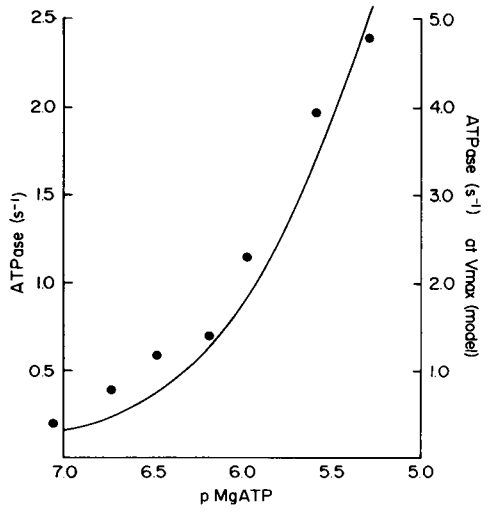

FIGURE 9 ATPase activity as a function of pMgATP. Data points are taken from Fig. 5 of Weber et al. (1969), using a conversion factor of 1 nmol myosin per mg myofibrillar protein (Hanson and Huxley, 1957). The solid curve is derived from the model. The rate is expressed in cycles of ATP hydrolysis per cross-bridge per second.

activated actomysin ATPase activity at high [MgATP] and the V_{max} of muscular contraction for muscles of various types has long been noted (Barany, 1967). The origin of this similarity was suggested by Eisenberg et al. (1980), also, to be their common dependence on the rate-limiting step in the cross-bridge cycle. In solutions of high [MgATP] the rate limiting step at V_{max} was suggested to be the transition of myosin from the refractory to the nonrefractory state (Eisenberg et al., 1980), in contrast to the situation described here at low levels of MgATP, where detachment appears to be rate limiting.

ATP Binding. The fraction of cross-bridges with myosin bound at different pMgATP, as predicted by the model, is shown in Fig. 10 along with data taken from Maruyama and Weber (1972) for the binding of ATP to actomyosin. Note that the good fit is only evident for a fraction of the cross-bridges (note that the ordinate of Fig. 10 spans the fraction between 0.3 and 1.0). This is because the cross-bridges cannot be bound near the extremities of the actin repeat distance (at +190 or −190 Å); this is a condition needed for calculating the n values (Fig. 8). Thus, cross-bridges in these regions will be free, and since we have used a very low dissociation constant ($K_S = 10^{-11}$) for ATP binding (Goody et al., 1977), there will always be some detached cross-bridges with ATP bound, at the values of pMgATP used in this study. It is clear from Fig. 10, however, that the model gives a realistic prediction of ATP binding to those cross-bridges associated with the actin filament. This is further support for the notion that the affinity of actomyosin for ATP is much less than that of acto-S1 for ATP.

It is clear from these results that under conditions of low MgATP the shortening characteristics of muscle are dominated by the detachment function g. This function describes two processes: the binding of ATP and the subsequent release of the cross-bridge. The binding constant of ATP for acto-S1 has been reported as being $\sim 10^7$ M^{-1} (Stein et al., 1979). If this were the binding constant at the site of detachment in contracting muscle and rapid equilibrium conditions prevailed, we would not expect to see an effect of MgATP concentration on contraction in the range of concentrations used here, since the actomyosin would be always nearly saturated with MgATP. If, on the other hand, 10^7 M^{-1} is characteristic of ATP binding to actomyosin at x = 80 Å, and the free energy associated with the binding of ATP to actomyosin is a function of x (Eisenberg and Greene, 1980), the apparent affinity of ATP for actomyosin near x = 0 (where nucleotide-free actomyosin appears) will be reduced. It is then quite feasible for the detachment rate to be first order with respect to [MgATP], as appears to be the case, and for there to be a significant fraction of the actomyosin without ATP bound even at fairly high levels of [MgATP].

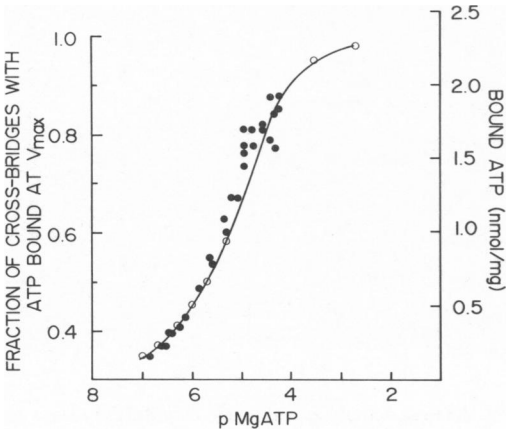

FIGURE 10 ATP bound to cross-bridges as a function of pMgATP. Data points (●) are taken from Fig. 3 of Maruyama and Weber (1972). Open circles (○) are values derived from the model.

Finally, the fact that a number of features of muscle shortening can be duplicated by this model does not mean that the model is necessarily correct even in its broadest conception. It is quite possible that a number of different formulations would have given the same or better results. The limited success of the present model does, however, show that the shortening properties of muscle at high pMgATP can be explained within the broad concepts of cross-bridge behavior currently held. Moreover, the model does offer an explanation for the most striking feature of the data: the pMgATP dependence of V_{max} and its similarity to the ATPase data of Weber et al. (1969).

The authors would like to acknowledge the assistance of Ms. Ann Swinford.

This work was supported by grants from the National Institutes of Health (HL25861), the Muscular Dystrophy Association, Surgical Associates of University of Wisconsin Hospitals, and the American Heart Association with funds contributed in part by the Wisconsin Affiliate. Dr. Moss is an Established Investigator of the American Heart Association.

Received for publication 31 August 1982 and in final form 7 December 1983.

REFERENCES

Bárány, M. 1967. ATPase activity of myosin correlated with speed of muscle shortening. *J. Gen. Physiol.* 50 (Suppl.):197–218.

Bendall, J. R. 1951. The shortening of rabbit muscles during rigor mortis: its relation to the breakdown of ATP and creatine phosphate and to muscular contraction. *J. Physiol. (Lond.).* 114:71–88.

Best, P. M., S. K. B. Donaldson, and W. G. L. Kerrick. 1977. Tension in mechanically disrupted mammalian cardiac cells: effects of magnesium adenosine triphosphate. *J. Physiol. (Lond.).* 265:1–17.

Bremel, R. D., and A. Weber. 1972. Cooperation within actin filament in vertebrate skeletal muscle. *Nat. New Biol.* 238:97–101.

Ebashi, S., M. Endo, and I. Ohtsuki. 1969. Control of muscle contraction. *Q. Rev. Biophys.* 2:351–384.

Eisenberg, E., and L. E. Greene. 1980. The relation of muscle biochemistry to muscle physiology. *Ann. Rev. Physiol.* 42:293–309.

Eisenberg, E., T. L. Hill, and Y. Chen. 1980. Cross-bridge model of muscle contraction. *Biophys. J.* 29:195–227.

Endo, M. 1964. The superprecipitation of actomyosin and its ATPase activity in low concentrations of ATP. *J. Biochem.* 55:614–622.

Fabiato, A., and F. Fabiato. 1975. Effects of magnesium on contractile activation of skinned cardiac cells. *J. Physiol. (Lond.).* 249:497–517.

Ferenczi, M. A., Y. E. Goldman, and R. M. Simmons. 1979. The relation between maximum shortening velocity and the magnesium adenosine triphosphate concentration in frog skinned muscle fibres. *J. Physiol. (Lond.).* 292:71P–72P.

Fung, Y. C. B. 1967. Elasticity of soft tissues in simple elongation. *Am. J. Physiol.* 213:1532–1544.

Godt, R. E. 1974. Calcium-activated tension of skinned muscle fibers of the frog: dependence on magnesium adenosine triphosphate concentration. *J. Gen. Physiol.* 63:722–739.

Goody, R. S., W. Hofmann, and G. H. Mannherz. 1977. The binding constant of ATP to myosin S1 fragment. *Eur. J. Biochem.* 78:317–24.

Gordon, A. M., A. F. Huxley, and F. J. Julian. 1966. The variation in isometric tension with sarcomere length in vertebrate striated muscle. *J. Physiol. (Lond.).* 184:170–192.

Guerriero, V., Jr., D. R. Rowley, and A. R. Means. 1981. Production and characterization of an antibody to myosin light chain kinase and intracellular localization of the enzyme. *Cell.* 27:449–458.

Hanson, G., and H. E. Huxley. 1957. Quantitative studies on the structure of cross-striated myofibrils. II. Investigations by biochemical techniques. *Biochim. Biophys. Acta.* 23:250–260.

Haselgrove, J. C. 1975. X-ray evidence for conformational changes in the myosin filaments of vertebrate striated muscle. *J. Mol. Biol.* 92:113–143.

Hill, T. L., and G. M. White. 1968. On the sliding-filament model of muscular contraction. IV. Calculation of force-velocity curves. *Proc. Natl. Acad. Sci. USA.* 61:889–896.

Huxley, A. F. 1957. Muscle structure and theories of contraction. *Prog. Biophys. Biophys. Chem.* 7:255–318.

Julian, F. J. 1971. The effect of calcium on the force-velocity relation of briefly glycerinated frog muscle fibers. *J. Physiol. (Lond.).* 218:117–145.

Julian, F. J., and R. L. Moss. 1981. Effects of calcium and ionic strength on shortening velocity and tension development in frog skinned muscle fibres. *J. Physiol. (Lond.).* 311:179–199.

Julian, F. J., R. L. Moss, and G. S. Waller. 1981. Mechanical properties and myosin light chain composition of skinned muscle fibers from adult and new-born rabbits. *J. Physiol. (Lond.).* 311:201–218.

Katz, B. 1939. The relation between force and speed in muscular contraction. *J. Physiol. (Lond.).* 96:45–64.

Kawai, M., and P. W. Brandt. 1976. Two rigor states in skinned crayfish single muscle fibers. *J. Gen. Physiol.* 68:267–280.

Marston, S. and A. Weber. 1975. The dissociation constant of the actin-heavy meromyosin subfragment-1 complex. *Biochemistry.* 14:3868–3873.

Maruyama, K., and A. Weber. 1972. Binding of adenosine triphosphate to myofibrils during contraction and relaxation. *Biochemistry.* 11:2990–2997.

Moss, R. L. 1979. Sarcomere length-tension relations of frog skinned muscle fibres during calcium activation at short lengths. *J. Physiol. (Lond.).* 292:177–192.

Moss, R. L. 1982. The effect of calcium on the maximum velocity of shortening in skinned skeletal muscle fibres of the rabbit. *J. Muscle Res. Cell Motil.* 3:295–311.

Mulvany, M. J. 1975. Mechanical properties of frog skeletal muscles in iodoacetic acid rigor. *J. Physiol. (Lond.).* 252:319–334.

Reuben, J. P., P. W. Brandt, M. Berman, and H. Grundfest. 1971. Regulation of tension in the skinned crayfish muscle fiber. I. Contraction and relaxation in the absence of Ca (pCa > 9). *J. Gen. Physiol.* 57:385–407.

Sillen, L. G., and A. E. Martell. 1964. Stability Constants of Metal-Ion Complexes. Special Publication No. 17. The Chemical Society, London. Second ed.

Spudich, J. A., H. E. Huxley, and J. T. Finch. 1972. Regulation of skeletal muscle contraction. II. Structural studies of the interaction of the tropomyosin-troponin complex with actin. *J. Mol. Biol.* 72:619–632.

Stein, L. A., R. P. Schwarz, P. B. Chock, and E. Eisenberg. 1979. Mechanism of actomyosin adenosine triphosphatase. Evidence that 5-triphosphate hydrolysis can occur without dissociation of the actomyosin complex. *Biochemistry.* 18:3895–3909.

Weber, A., R. Herz, and I. Reiss. 1969. The role of magnesium in the relaxation of myofibrils. *Biochemistry.* 8:2266–2270.

White, D. C. S. 1970. Rigor contraction and the effect of varions phosphate compounds on glycerinated insect flight and vertebrate muscle. *J. Physiol. (Lond.)* 208:583–605.

Wood, D. S., J. Zollman, J. P. Reuben, and P. W. Brandt. 1975. Human skeletal muscle: properties of the chemically skinned fiber. *Science (Wash. DC).* 187:1075—1076.